Orbital: The Electronic Journal of Chemistry
journal homepage: www.orbital.ufms.br
ISSN 1984-6428

| Vol 10 || No. 1 || Special Issue January 2018 |

Full Paper

Low Temperature Synthesis of Several Titanium Dioxide Solid Solutions through the Sol-Gel Method

Natali Amarante da Cruz*[a], Silvanice Aparecida Lopes dos Santos[b], Lincoln Carlos Silva de Oliveira[b], Rafael Aparecido Ciola Amoresi[c], Maria Aparecida Zaghete[c], Rony Gonçalves Oliveira[d], Luis Humberto da Cunha Andrade[e], Alberto Adriano Cavalheiro[a]

[a]*LIMAN - CDTEQ - Universidade Estadual de Mato Grosso do Sul, R. Emílio Mascoli, 275 - Jardim Vale Encantado, 79950-000, Naviraí - MS, Brazil.*
[b]*INQUI - Universidade Federal de Mato Grosso do Sul, Av. Senador Filinto Muller, 1555 – Ipiranga, 79064-470, Campo Grande, MS, Brazil.*
[c]*LIEC - IQCar - Universidade Estadual Paulista, Rod. Araraquara-Jaú Km, Bairro Machados, 14800-901, Araraquara, SP, Brazil.*
[d]*CEPEMAT - Universidade Estadual de Mato Grosso do Sul, R. Emílio Mascoli, 275 - Jardim Vale Encantado, 79950-000, Naviraí - MS, Brazil.*
[e]*CERNA - Universidade Estadual de Mato Grosso do Sul, R. Emílio Mascoli, 275 - Jardim Vale Encantado, 79950-000, Naviraí - MS, Brazil.*

Article history: Received: 30 June 2017; revised: 11 July 2017; accepted: 15 July 2017. Available online: 29 January 2018.
DOI: http://dx.doi.org/10.17807/orbital.v10i1.1038

Abstract: Titanium dioxide powders constituted by anatase single phase are very useful to understand several properties of that semiconductor applied as photocatalyst material. In addition, the reconstructive transformation involved in the anatase-to-rutile phase transition is also dependent of compositional and structural characteristics, which is consequence of the xerogel precursors. In this work, it was provided some structural investigation and the thermal event associated to different compositions of titanium dioxide xerogel samples obtained by Sol-Gel method. It was prepared two different doped-sample sets, one with bared titanium dioxide matrix and other with 10 mol% of zirconium-silicon one, and both sample sets were submitted to doping with 2 mol% of cation pairs, taking in account the ionic radii and oxidation states. The small and pentavalent vanadium cation was combined with trivalent and bigger lanthanum and bismuth ones, in order to provide non strained unit cell making an average values for ionic radii and oxidation states, taking in account the tetravalent titanium cation. By thermal analysis, X-ray diffractometry, FTIR and Raman spectroscopies it was possible to demonstrate the insertion of bigger dopants as lanthanum and bismuth, as well as the smaller one as vanadium, which are usually dopants not supported in isolated forms were successfully incorporated to anatase phase when combined as expected in previous composition design stage.

Keywords: anatase phase; composition design; XRD; FTIR; raman

1. INTRODUCTION

Advanced ceramic materials are useful for uncountable purposes and the semiconductors are special type applied mainly as photonic devices. Titanium dioxide is one semiconductor materials easily excited under low energetic ultraviolet radiation, such as 3.2 eV (UV-A region), but other characteristics such as high resistance to lixiviation in a wide range of pH and absence of toxicity, make them the most promising heterogeneous photocatalyst applied to water treatment, in special those destined to human consumption [1-3].

The titanium dioxide possesses two stable phases in ordinary conditions, named anatase and rutile ones. During the semiconductor excitation by UV radiation, the generated electron-hole pairs are transferred toward aqueous medium, which is essential to generates the oxidative radical species in aqueous media and initiate the water treatment by advanced oxidation process. Several dopants have been investigated in recent years in order to improve several aspects of that photocatalyst semiconductor, but high amounts of structural defects in anatase phase acts as recombining centers, which harms the photocatalytic performance. Thus, the anatase phase

*Corresponding author. E-mail: nataliamarante19@gmail.com

must be subjected to crystallization in temperatures below 600 ºC to avoid the anatase-to-rutile phase transition [4-9].

The use of chemical methods for the titanium dioxide synthesis has shown impressive ability to obtain bare and doped anatase single phase at low temperatures, such as 450 ºC for powder samples and 250 ºC for thin films. Even so, the increasing in temperature in order to promote the defect eliminations above 600 ºC ends up leading to irreversible anatase-to-rutile phase transition, which lead us to investigate the stabilization of anatase phase at higher temperature than 600 ºC, as reported in previous work [10,11]. In those works, the stabilized titanium dioxide samples were submitted to crystallization until 900 ºC and no trace of rutile phase was observed.

The isolated forms of those dopants does not present the same behavior, as related by others researchers [12-17]. The same design logic used to propose the anatase phase stabilization with zirconium-silicon dopant pair is now used to propose the additional dopant pair insertion. Different from tetravalent zirconium and silicon cations, similar to the titanium one, now we propose the insertion of equimolar amounts of trivalent and pentavalent cations but keeping the combination of bigger and smaller cations. Thus, in order to investigate the behavior of the stabilized anatase titanium dioxide phase when new other dopants are inserted in material, we carry out the preparation of 10 mol% zirconium-silicon doped-titanium dioxide powder by sol-gel method using as blank sample a non-doped sample prepared in the same conditions. Then, the dopant pairs of bismuth and vanadium and lanthanum- and vanadium were inserted at 2 mol% in both matrixes and the obtained precursors were characterized by thermal analysis, X-ray diffraction, FTIR and Raman spectroscopies.

2. MATERIAL AND METHODS

The material samples were synthesized through the sol-gel method following subsequent steps. Firstly, the titanium tetraisopropoxide IV (97 %, Aldrich) was drop wised into acetic acid (R.G., Dinamica) to form a metallic acetate complex with stoichiometry MeL_4 and stirred for 30 min. For zirconium-silicon stabilized titanium dioxide matrixes, tetraethyl orthosilicate (98 %, Aldrich) and zirconium propoxide (70 %, Aldrich) were drop wised in sequence, following 30 min more under stirring. Both solutions were diluted with ethylic alcohol (R.G., Dinamica) at 50 % in volume and homogenized for 30 min more for complete homogenization.

The dopant precursors were added through the aqueous solutions, where the molar ratios between water and ceramic composition were 10 to 1. All of the dopant solutions were prepared in separate flasks by dissolving aliquots of ammonium metavanadate (R.G., Vetec) in water and 3 drops of ammonium hydroxide (R.G., Vetec). In sequence, the lanthanum oxide (R.G., Vetec) and basic bismuth subnitrate (R.G., Dinamica) were dissolved with nitric acid (R.G., Vetec) in separate flaks and finally added to different solutions, in order to result in six different compositions, as show in Table I. After stirring for 1 hour more, each batch solution was let to during 24 hours at room temperature, dried at 100 ºC for 24 h in oven, milled and dried again at 100 ºC for 24 h more.

The thermal analysis was taken in TA Instruments equipment under synthetic air flow of 60 mL min^{-1} and heating rate of 10 ºC min^{-1}. The X-ray diffraction patterns were taken from at room temperature from 20 to 80 º (2-theta) degrees at 1º (2-theta)/min by using Siemens equipment, model D5005, with K-alpha Cu radiation. The Raman spectra measurements were taken using spectrometer DU420_DD model, B&W Tek e Andor Technologies, with 532 nm line laser as excitation source. FTIR spectra were taken using Thermo Nicolet - photoacoustic detector, from 400 to 4000 cm^{-1}.

Table 1. Description and nominal compositions for investigated doped and stabilized titanium dioxide samples.

Samples	Nominal Composition
Pure TiO_2 sample - TP	TiO_2
2 mol% bismuth-vanadium doped-TP sample - BVT	$(Bi,V)_{0,02}Ti_{0,98}O_2$
2 mol% lanthanum-vanadium doped-TP sample - LVT	$(La,V)_{0,02}Ti_{0,98}O_2$
10 mol% zirconium-silicon stabilized TiO_2 sample - ZST	$(Zr,Si)_{0,1}Ti_{0,9}O_2$
2 mol% bismuth-vanadium doped-ZST sample - BVZST	$(Bi,V)_{0,02}(Zr,Si)_{0,1}Ti_{0,88}O_2$
2 mol% lanthanum-vanadium doped-ZST sample - LVZST	$(La,V)_{0,02}(Zr,Si)_{0,1}Ti_{0,88}O_2$

3. RESULTS AND DISCUSSION

In Figure 1 is shown the aspects of xerogel sample as a function of stabilization and modification. The colors are function of contribution of typical aqueous complex colors of chromophore cations, such as vanadium and bismuth ones, which possess yellowish contribution xerogel samples. However, for zirconium stabilized samples, the color intensities are attenuated, which indicates that structural and chemical changes are occurring in the samples.

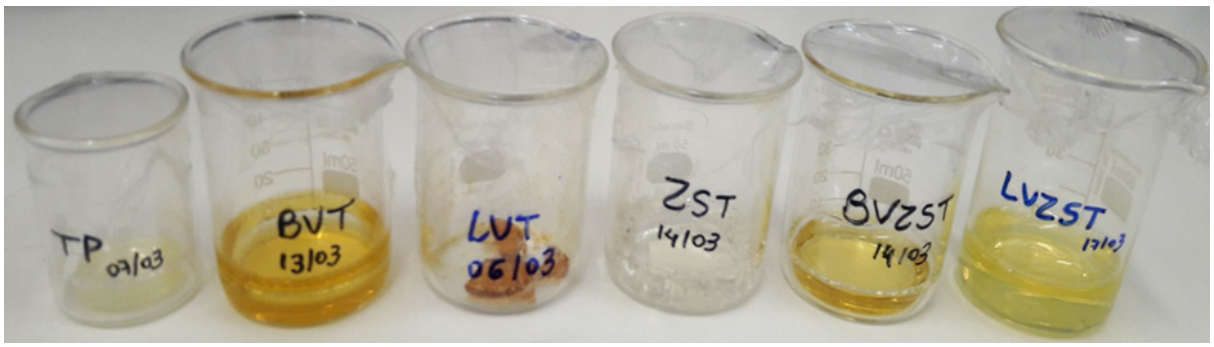

Figure 1. Xerogel samples dried at room temperature for 24 hours, comparing no stabilized and zirconium-silicon stabilized titanium dioxide samples.

In Figure 2 is shown the thermal analyses for all of the xerogel samples. There are three main thermal events in all of the samples, designated as I, II and III in all of the DTG curves. The first one (I) is related to volatilization of residual compounds below 100 ºC and present endothermic peak in DSC curves. No doped samples (TP and ZST) present lower weight losses (8-9%) for that event, as visualized in Fig. 2.a, which is probably due to lower stability for titanium, zirconium, and silicon carboxylates, different from doped samples visualized in Figs 2.b and 2.c., which present around 50 % more weight losses in that event (11-12 %) due the stable metallic hydrates for bismuth, lanthanum and vanadium cations.

The second and third thermal events are start above 200 ºC and are related to hydroxyl group condensation in order to forming cross-linked metal-oxygen bonds [18]. Is very probable the first condensation stage at lower temperature is related to formation of vicinal cross-link bonds in the same nucleus, while the second one is related to formation of cross-link bonds among the nuclei [19]. Those exothermic events are strongly influenced by doping process and vanadium hydroxyl groups seem to be less stable than other metal hydroxides [10].

However, the zirconium-silicon stabilized matrix promotes the attenuation of those differences, in similar mode to the verified behavior for non-doped samples, once the zirconium hydrates are less stable than titanium ones [20]. DTG peaks for stages II and III appear attenuated and displaced 30 ºC to higher temperatures for doped and stabilized samples if compared to the same DTG peaks for doped only ones. Those results can be related to the existence of more interconnected anatase particles in stabilized samples, which hinder the dehydroxylation process along the temperature increasing.

By observing the X-ray diffraction patterns for these samples in Figure 3, it is possible to see the stabilized samples with zirconium-silicon (dotted lines in XRD patterns) lead to low crystalline structures due the low intense peaks for all reflections planes, according the JCPDS file 71-11166 [21]. However, that low crystallinity for stabilized samples is less evident for LVSZT sample, when compared to LVT one, which permits to infer the lanthanum acts to order the anatase structure.

The most recent results obtained by our research group (not published yet) has shown that lanthanum-vanadium dopant pair is able to stabilizes the anatase phase up to 800 ºC with the same crystallinity of rutile ones. Thus, we can to affirm that dopant pair is a good inducer of anatase phase crystallization still at low temperature and even in a matrix stabilized with zirconium and silicon, known as crystallinity reducing [11].

In Figure 4 are shown the Raman spectra for all of the xerogel samples. The Raman spectra obtained from green laser at 532 nm showed the stabilized matrixes generate broader bands than no stabilized ones, independent of dopant insertion, which can be related to different energetic level for electronic transitions. However, only TP sample possesses typical Raman spectra for anatase TiO_2

crystalline sample, according the literature [22-24]. Nevertheless, the doped samples lead to less attenuation of the band intensities when the material is only stabilized with zirconium-silicon, but no doped.

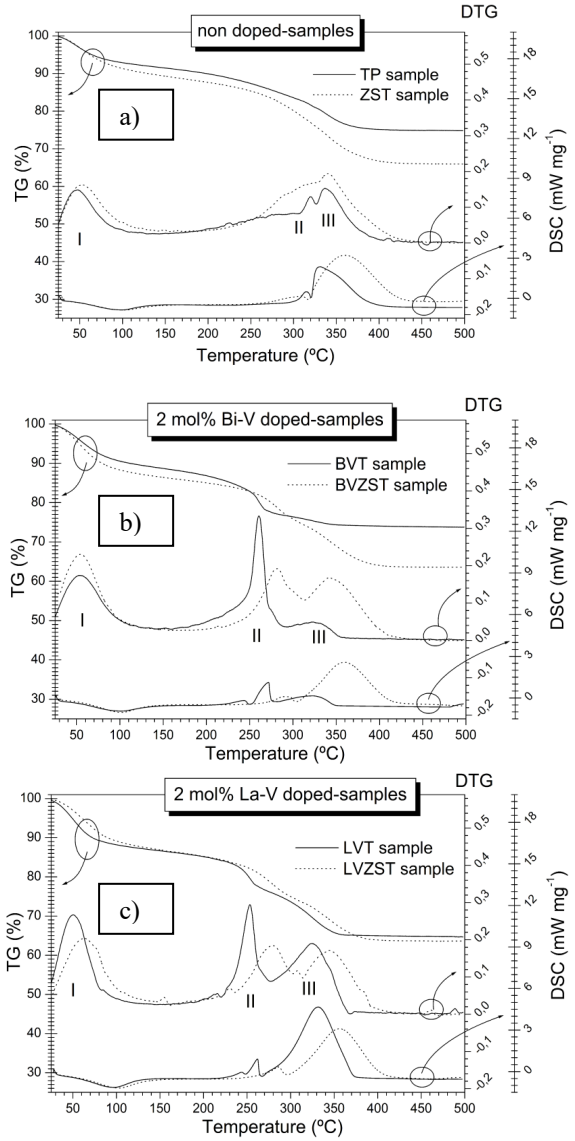

Figure 2. Thermal analysis for several dried samples at 100 ºC for 24 hours, comparing no stabilized and zirconium-silicon stabilized titanium dioxide samples: a) non doped, b) Bi-V dopes and c) La-V doped samples.

The typical Raman spectrum for high crystalline anatase structure should present one A1g band localized close to 520 cm^{-1}, two B1g bands localized close to 400 cm^{-1} and also at 520 cm^{-1} in overlapping with A1g band and finally, three Eg bands localized close to 150 cm^{-1}, 200 cm^{-1} and 640 cm^{-1}, once the B2u vibrational mode is silent. In fact, those low crystallized and stabilized structures presents two first Eg bands displaced to higher wavenumbers, close to 200 and 300 cm^{-1}, which show the stabilization process by insertion of zirconium and silicon dopant pair makes the M-O bonds energetic levels for the electronica transition.

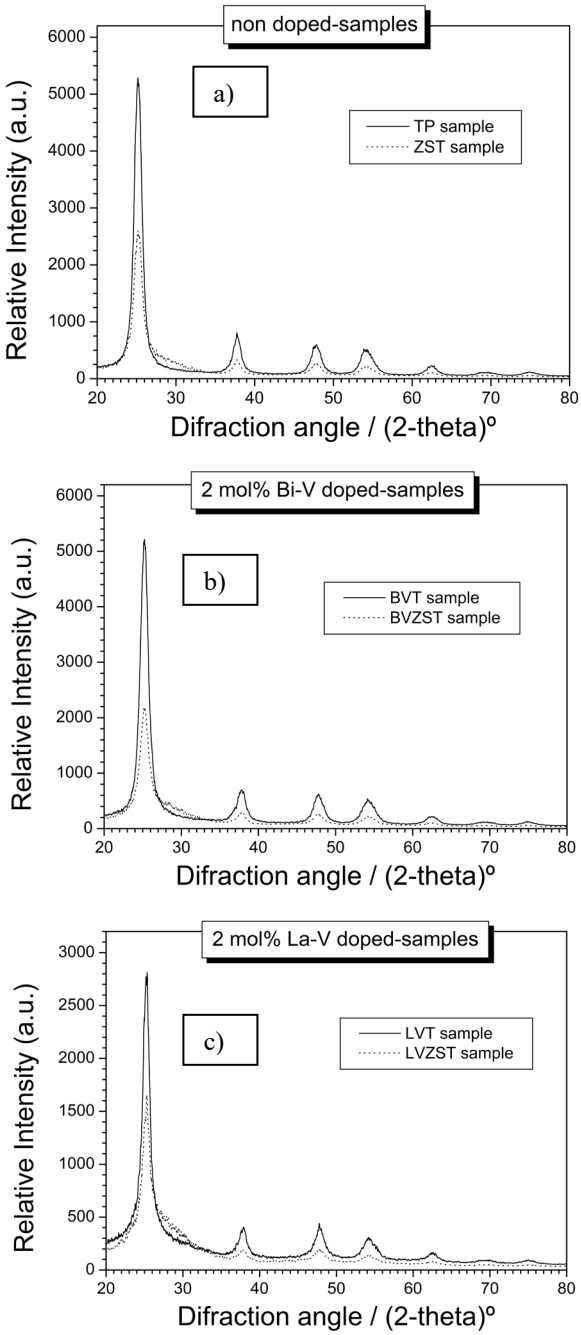

Figure 3. X-ray diffraction patterns for zirconium-silicon stabilized and no stabilized titanium dioxide xerogel samples: a) no doped, b) Bi-V doped and c) La-V doped.

Finally, the appearing of three bands at 900, 1000, and 1150 cm^{-1} is related to metallic hydroxyl species bound directly to the anatase nuclei surface

[25]. These terminal hydroxyl groups is more evident for stabilized samples, but is reduced for lanthanum-vanadium doped sample LVZST if compared to no stabilized correlate sample LVT. That result is coherent with X-ray results, once the more amounts of terminal groups on anatase nuclei surface causes a structural long range disordering.

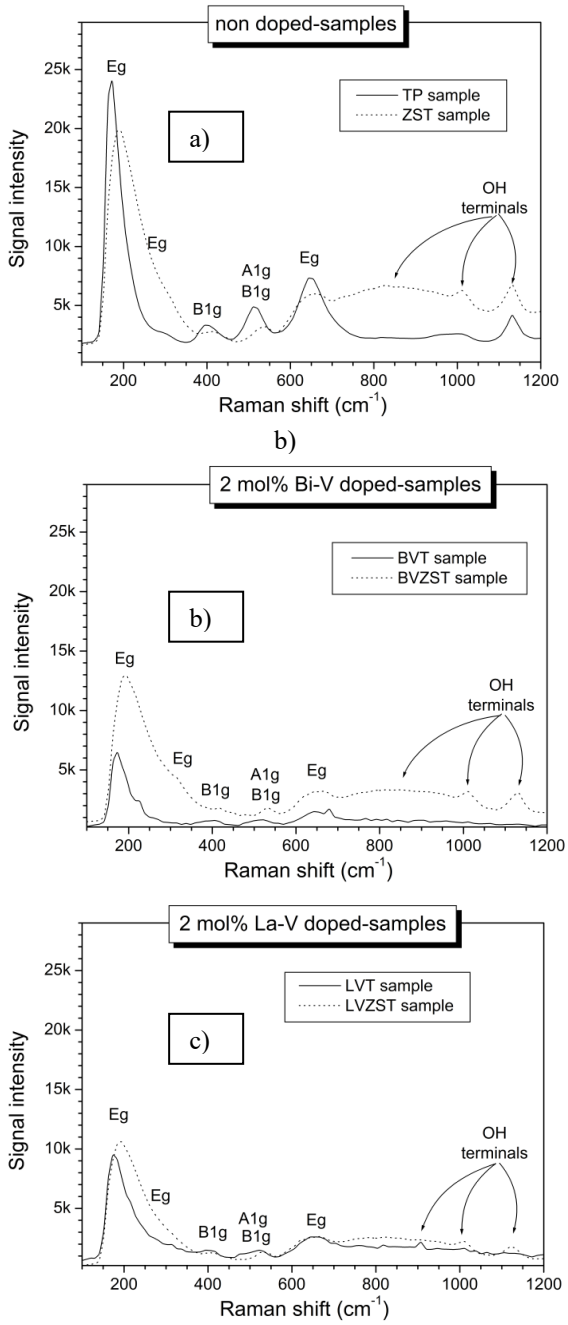

Figure 4. Raman spectra for zirconium-silicon stabilized and no stabilized titanium dioxide xerogel samples: a) no doped, b) Bi-V doped and c) La-V doped.

In Figure 5 are shown the FTIR spectra and in Table 2 the collected band position for these samples.

No substantial changes were verified among the samples concerning structure energies. Only the noticeable M-OH stretching vibration originated from metal hydroxide close to 3000 cm^{-1} is observed for LVZST sample, followed by the band IV at 1050 cm^{-1} associated to freeze water molecule bonded on nuclei surface [22]. The positions of each band can be view in detail on Table 2.

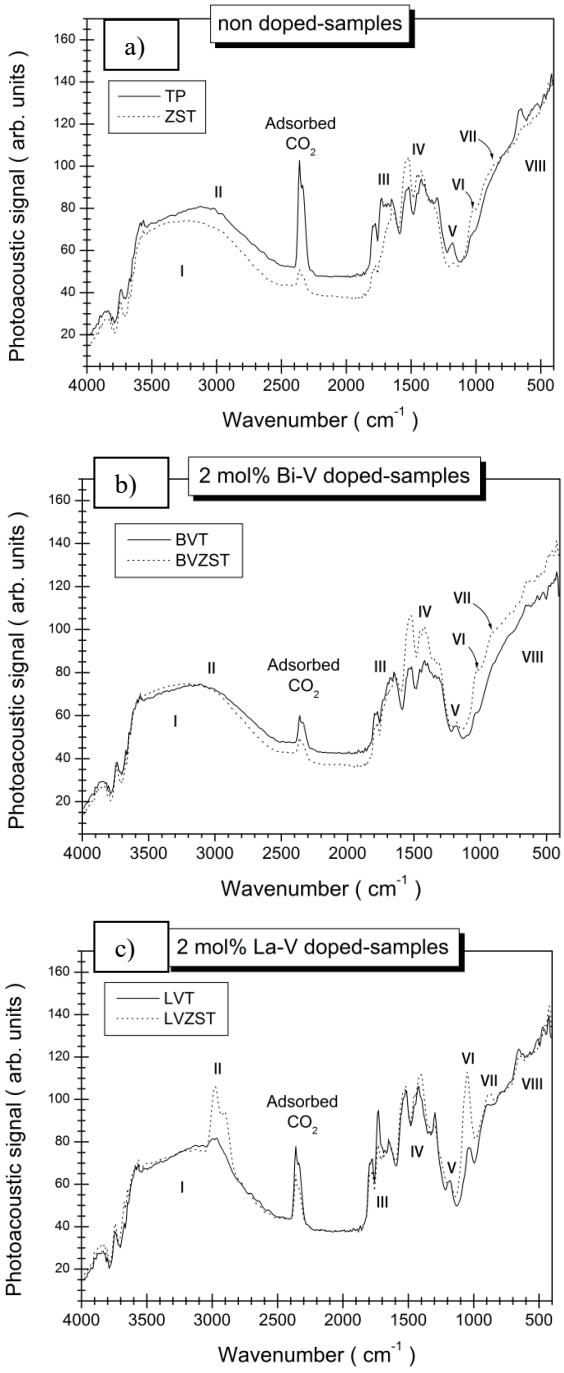

Figure 5. FTIR spectra for zirconium-silicon stabilized and no stabilized titanium dioxide xerogel samples: a) no doped, b) Bi-V doped and c) La-V doped.

Table 2. Main identified bands in FTIR spectra for zirconium-silicon stabilized and no stabilized titanium dioxide xerogel samples.

Band	Identification of bands	Wavenumber (cm^{-1})					
		Not stabilized			ZS stabilized		
		TP	BVT	LVT	ZST	BVZST	LVZST
I	O-H stretching vibration (H-bridge from adsorbed water)	3260	3300	3220	3260	3300	3220
II	M-OH stretching vibration (metal hydroxide)	3020	3050	3000	3020	3050	3000
III	C=O stretching vibrations	1730	1650	1730	1650	1650	1740
IV	O-H deformation vibration	1520	1420	1420	1520	1420	1400
V	O-H deformation and C-O stretching vibration interaction	1180	1180	1180	1170	1180	1180
VI	Freeze water vibration	960	950	1040	1000	1030	1050
VII	Ti(Si,Zr)-OH stretching vibration	840	830	900	840	910	870
VIII	Metal-oxide skeletal vibration	660	660	650	660	660	660

4. CONCLUSION

In conclusion, it was observed the doping pair of zirconium and silicon changes the xerogel characteristics, mainly the terminal hydroxyl groups, which seems to be more abundant if compared to no stabilized samples. Consequently, cross-link bonds among the anatase nuclei are enhanced during leads to the structural long-range disordering. The bigger dopant cations like bismuth and lanthanum has compensatory effect on the lattice distortion and seems does not affect the crystallinity as much as the zirconium-silicon dopant pair seems to do.

5. ACKNOWLEDGMENTS

The authors thank FUNDECT-MS, CNPq, and CAPES for financial supports.

6. REFERENCES AND NOTES

[1] Castro, Y.; Arconada, N.; Durán, A. *Bol. Soc. Esp. Cerám. Vidr*. **2015**, *54*, 11. [CrossRef]

[2] Chenga, X.; Yu, X.; Xinga, Z.; Wan, J. *Energy Procedia* **2012**, *16*, 598. [CrossRef]

[3] Ibrahim, S. A.; Ahmid, M. N. *Mater. Sci. Forum* **2017**, *888*, 435. [CrossRef]

[4] Fagan, R.; McCormack, D. E.; Hinder, S. J.; Pillai, S. C. *Mater Design*. **2016**, *96*, 44. [CrossRef]

[5] Haque, F. Z.; Nandanwar, R.; Singh, P. *Optik Int. J. Light Elect. Opt*. **2017**, *128*, 191. [CrossRef]

[6] Muff, J.; Simonsen, M. E.; Sogaard, E. G. *J. Environ. Chem. Eng*. **2017**, *5*, 3201. [CrossRef]

[7] Singh, S.; Dey, S. S.; Singh, S.; Kumar, N. *Materi Today: Proc*. **2017**, *4*, 3300. [CrossRef]

[8] Saleiro, G. T.; Cardoso S. L.; Toledo R.; Holanda, J. N. F. *Cerâmica*. **2010**, *56*, 162. [CrossRef]

[9] Hailu, S. L.; Nair, B. U.; Redi-Abshiro, M.; Aravindhan, R.; Diaz, I.; Tessema, M. *J. Porous Mater*. **2015**, *22*, 1363. [CrossRef]

[10] Cavalheiro, A. A. Oliveira, L. C. S.; Santos, S. A. L. In: Titanium Dioxide, *InTech Book*. **2017**, *3*, 63. [Link]

[11] Cruz, N. A.; Cavalheiro, A. A.; Stropa, J. M.; Favarin, L. R. V.; Machulek, A.; Oliveira, L. C. S.; Amoresi, R. A. C.; Zaghete, M. A. *IJLRET* **2017**, *3*, 428. [Link]

[12] Wang, C. Li.; Hwang W. S.; Chu H. L.; Lin H. J.; Ko H. H.; Wang M. *Chin. Ceram. Int*. **2016**, *42*, 3136. [CrossRef]

[13] Guesh, K.; Mayoral, Á.; Márquez-Álvarez, C.; Chebude, Y.; Díaz, I. *Micro Meso Mater*. **2016**, *225*, 88. [CrossRef]

[14] Guesha, K.; Márquez-Álvarez, C.; Chebude, Y.; Díaz, I. *Appl. Surf. Sci*. **2016**, *378*, 473. [CrossRef]

[15] Marzec, A.; Radecka, M.; Maziarz, W.; Kusior, A.; Pedzich, Z. *J. Eur. Ceram. Soc*. **2016**, *36*, 2981. [CrossRef]

[16] Harraz, F. A.; Abdel-Salam, O. E.; Mostafa, A. A.; Mohamed, R. M.; Hanafy, M. J. *Alloys Comp*. **2013**, *551*, 1. [CrossRef]

[17] Smirnova, N.; Petrik, I.; Vorobets, V.; Kolbasov, G.; Eremenko, A. *Nano Res. Lett*. **2017**, *12*, 1. [CrossRef]

[18] Hart, J. N.; Bourgeois, L.; Cervini, R.; Cheng, Y.-B.; Simon, G. P.; Spiccia, L. *J. Sol-Gel Sci. Tech*. **2007**, *42*, 107. [CrossRef]

[19] Xu, M.; Shao, S.; Gao, B.; Lv, J.; Li, Q.; Wang, Y.; Wang, H.; Zhang, l.; Ma, Y. *ACS Appl. Mater. Interfaces*. **2017**, *9*, 7891. [CrossRef]

[20] De Carli, E. F.; Santos, M.; Cruz, N. A.; Manfroi, D. C.; Stropa, J. M.; Oliveira, L. C. S.; Zaghete, M. A.; Cavalheiro, A. A. *Mater Sci. Forum*. **2017**, *881*, 18. [CrossRef]

[21] JCPDS - Joint Committee on Powder Diffraction Standards/International Center for Diffraction Data, Pennsylvania, Powder Diffraction File 2003.

[22] Nolan, N. T.; Seery, M. K.; Pillai, S. C. *J. Phys. Chem. C*. **2009**, *113*, 16151. [CrossRef]

[23] Šćepanović, M. J.; Grujić-Brojčin, M.; Dohčević-Mitrović, Z. D.; Popović, Z. V. *Sci. Sint*. **2009**, *41*, 67. [CrossRef]

[24] Bagheri, S.; Shameli, K Hamid, S. B. A. *J. Chem*. **2013** *Article ID 848205*. [CrossRef]

[25] Rodella, C. B.; Franco, R. W. A.; Magon, C. J.; Donoso, J. P. Nunes, L. A. O.; Saeki, M. J.; Aegerter, M. A.; Sargentelli, V.; Florentino, A. O. *J. Sol-Gel Sci. Tech*. **2002**, *25*, 83. [CrossRef]